Supporting Information

Heteroaggregation of Multiwalled Carbon Nanotubes and Hematite Nanoparticles: Rates and Mechanisms

KHANH AN HUYNH,[†] J. MICHAEL MCCAFFERY,[‡] AND KAI LOON CHEN[*, †]

[†]Department of Geography and Environmental Engineering, Johns Hopkins University, Baltimore, Maryland 21218-2686

[‡]The Integrated Imaging Center, Department of Biology, Johns Hopkins University, Baltimore, Maryland 21218-2686

(*E-mail: kailoon.chen@jhu.edu)

Contents

Additional Details on Materials and Methods

Preparation of Multiwalled Carbon Nanotubes and Nanotube Stock Suspension. The procedure for the preparation of multiwalled CNTs and CNT stock suspension was reported in our earlier publication.[1] Pristine multiwalled CNTs (PD15L5-20, NanoLab Inc., Waltham, MA) were refluxed in a 3:1 volume mixture of 98% sulfuric acid (H_2SO_4) and 69% nitric acid (HNO_3) at 70 °C for 8 h. The concentration of pristine CNTs in the acid mixture was 12.5 mg/mL. To remove residual acids, metallic byproducts, and amorphous carbon, the oxidized CNTs were cleaned through repeated cycles of dilution with deionized (DI) water, ultracentrifugation at 1850*g* (Powerspin LX, Unico, Dayton, NJ) for 5–10 min, and decantation of supernatant until the pH and resistivity of the supernatant was 5.5 and greater than 0.5 MΩ·cm, respectively. The cleaned CNTs were then dried in an oven overnight at 100 °C and pulverized using a ball-mill (MM200, Retsch, Germany) for 15 min. After pulverization, the CNT powder was stored in a capped glass vial in the dark at room temperature. To prepare a CNT stock suspension, an ultrasonic bath (Branson 150R-MT, output power 70 W, frequency 40 kHz) was used to disperse ca. 0.5 mg of CNT powder in 200 mL of DI water (Millipore, MA) for 20 h. To remove CNT clusters that still remained in the suspension after ultrasonication, the suspension was centrifuged at 1400*g* (Avanti centrifuge J-20 XPI, Beckman Coulter Inc., Brea, CA) for 5–10 min. The supernatant was then carefully transferred into a clean Pyrex bottle and stored in the dark at 4 °C.

Transmission Electron Microscopy Imaging of Carbon Nanotubes and Hematite Nanoparticles. A transmission electron microscope operating at 100 kV (TEM, FEI Tecnai 12 TWIN) was used to examine the structures and determine the length and size distributions of CNTs and hematite nanoparticles (HemNPs). A 5–10 μL drop of either CNT or HemNP suspension was deposited and dried on a carbon-coated copper TEM grid prior to being examined by the TEM. The length distribution of CNTs and size distribution of HemNPs were determined by measuring the lengths and diameters of over 500 randomly selected nanotubes and HemNPs, respectively (iTEM software, Olympus Soft Imaging Solutions GmbH, Münste, Germany). Additional high-resolution TEM (HR-TEM) images of CNTs and HemNPs were captured with a Philips CM300 FEG TEM. For HR-TEM imaging, CNT and HemNP samples were deposited and dried on lacey carbon-coated TEM copper specimen grids before being observed by TEM at 300 kV.

Electrophoretic Mobility Measurements. The electrophoretic mobilities (EPMs) of CNTs and HemNPs were measured with a ZetaPALS analyzer (Brookhaven, Holtsville, NY) at 0.1 mM NaCl and pH 5.2. All measurements were conducted at 25 °C. The concentrations of CNT and HemNP suspensions used for the EPM measurements were 0.56 mg/L total organic carbon (TOC) and 0.88 mg/L, respectively. The EPMs of these nanoparticles were also determined in the presence of humic acid with concentrations ranging from 0.15 to 500.00 μg/L TOC. Four nanoparticle samples were prepared for each solution chemistry and 10 EPM measurements were performed on each sample.

Time-Resolved Dynamic Light Scattering Measurements. For the homoaggregation experiments, homoaggregation was induced by introducing a predetermined volume of NaCl stock solution into a borosilicate vial that contained a diluted suspension of either CNTs or HemNPs. The suspension was briefly mixed (< 3 s) using a vortex mixer (Vortex Genie 2, Fisher) operated at its maximum setting and the vial was immediately inserted into the goniometer for DLS measurements. The final suspensions had a total volume of 1 mL with either a CNT concentration of 83.46 μg/L TOC or HemNP concentration of 0.44 mg/L. For CNT homoaggregation experiments, the laser power and detector aperture of the light scattering setup were adjusted to 3 W and 400 μm, respectively. In the case of HemNP homoaggregation experiments, the laser power and detector aperture of the light scattering setup were adjusted to 2 W and 200 μm, respectively. All vials were only used once. Before use, they were soaked overnight in a cleaning solution (Extran MA01, Merck KGaA, Darmstadt, Germany), rinsed with copious DI water, and dried in an oven under dust-free conditions.

For the heteroaggregation experiments performed in the absence of humic acid, heteroaggregation between CNTs and HemNPs was induced by adding a predetermined volume of CNT stock suspension into a vial containing a diluted HemNP suspension prepared with a NaCl solution. Similar to HemNP homoaggregation, an incident laser power of 2 W and a detector aperture of 200 μm were employed to determine the heteroaggregation rates through DLS measurements. The HemNP and NaCl concentrations of the final suspensions were 0.44 mg/L and 0.1 mM, respectively. The CNT concentrations in the final suspensions were varied from 1.11 to 27.82 μg/L TOC, resulting in the CNT/HemNP mass concentration ratios (CNT/HemNP ratios) to range from 0.0025 to 0.0632. The TOC content of CNTs was used for the calculation of the CNT/HemNP ratios.

For the heteroaggregation experiments performed in the presence of humic acid, a premeasured volume of humic acid stock solution, followed by a premeasured volume of NaCl stock solution, was introduced into a vial containing a diluted HemNP suspension. Following that, a premeasured volume of CNT stock suspension was introduced into the mixture. In these experiments, the final calculated humic acid concentrations ranged from 0.15 to 500.00 μg/L TOC. The final concentrations of HemNPs, CNTs, and NaCl were the same as those used for the heteroaggregation experiments in the absence of humic acid.

Determination of Homoaggregation Kinetics. At the early stage of homoaggregation, the aggregation rate constant, *k*, is proportional to the initial rate of change of the homoaggregate hydrodynamic diameter, D_h:[2]

$$k \propto \frac{1}{N_0}\left(\frac{dD_h(t)}{dt}\right)_{t\to 0} \tag{S1}$$

where t is time and N_0 is the initial primary particle concentration. The value of $\left(dD_h(t)/dt\right)_{t\to 0}$ was determined by performing a linear least-square analysis on the initial increase in D_h with t. For most NaCl concentrations, this analysis was performed over a time period in that D_h increased to 2.0 and 1.3 times of the initial hydrodynamic diameters of CNTs and HemNPs, respectively. However, at low NaCl concentrations, D_h did not reach the desired values due to slow aggregation and the analysis was performed over 45 min instead. For all analyses, the *y*-intercept of the fitted line did not exceed 12 and 5 nm in excess of the initial hydrodynamic diameters of CNTs and HemNPs, respectively.

The homoaggregation kinetics of CNTs and HemNPs were quantified using the attachment efficiency, α, that is calculated by normalizing the homoaggregation rate constant at the electrolyte concentration of interest, *k*, to that obtained under favorable aggregation condition, k_{fast}:[2-5]

$$\alpha = \frac{k}{k_{fast}} = \frac{\frac{1}{N_0}\left(\frac{dD_h(t)}{dt}\right)_{t\to 0}}{\frac{1}{(N_0)_{fast}}\left(\frac{dD_h(t)}{dt}\right)_{t\to 0,fast}} \tag{S2}$$

The terms with subscript "fast" refer to favorable conditions. The critical coagulation concentrations (CCCs) of CNTs and HemNPs can then be derived by determining the

intersections of the extrapolations through the reaction-limited and diffusion-limited regimes and used to quantify the colloidal stability of both nanoparticles.[3]

Cryogenic Transmission Electron Microscopy. Cryo-TEM was employed to examine the heteroaggregate structures formed at CNT/HemNP ratios of 0.0025, 0.0316, and 0.1265. The heteroaggregate suspensions were prepared in the same solution chemistry as that used for the heteroaggregation experiments (0.1 mM NaCl and pH 5.2) ca. 15 minutes before the vitrification process. CNT and HemNP concentrations used for cryo-TEM imaging were 10 times of the concentrations used for heteroaggregation experiments to allow for the formation of a reasonable number of heteroaggregates on each TEM grid. In addition, homoaggregates of CNTs prepared at a concentration of 1.25 mg/L TOC and a solution chemistry of 500 mM NaCl were observed with cryo-TEM 15 min after the onset of homoaggregation.

Lacey carbon-coated TEM copper grids were first ionized in a high vacuum evaporator (Denton 502A, Moorestown, NJ) for 30 s to increase the hydrophilicity of the grid surfaces. The ionized grid was then placed into a temperature/humidity controlled chamber of an automated vitrification robot (Vitrobot^{TM}) (FEI Vitrobot Mark IV, Hillsboro, OR) for specimen vitrification. The temperature and relative humidity of the chamber were maintained at 22 °C and > 90 %, respectively. 10 μL of suspension containing the aggregates of interest was deposited on the ionized grid; and the Vitrobot^{TM} then blotted the grid with filter paper to remove excess water. The high humidity minimizes the evaporation from the film of water (ca. 100–200 nm in thickness) on the grid after blotting, while the ionization of the grid promotes spreading of the thin water layer uniformly on the grid surface. After blotting, the specimen was rapidly plunged into a cryogen reservoir containing liquid ethane that was cooled by liquid nitrogen. The blotting and plunging were done automatically by the Vitrobot^{TM} with the predefined blotting and plunging parameters presented in Table S1. With the combination of these parameters and grid ionization, we reproducibly obtained a thin and uniform layer of vitreous ice containing aggregates of interest after vitrification.

After plunging into liquid nitrogen-cooled ethane, the vitreous specimen was quickly transferred to liquid nitrogen and subsequently transferred into a cryo workstation filled with liquid nitrogen (Gatan 626 workstation, Pleasanton, CA). The specimen was then placed in the tip of the cryo holder (Gatan 626 70° single tilt liquid nitrogen holder, Pleasanton, CA) and inserted into the TEM. Different from the standard holder used in conventional TEM, the cryo

holder has a shutter to shield the frozen hydrate specimen when it is being transferred into the TEM. The cryo holder also has a dewar, which contains sorb material (zeolite) internally at its base, and is filled with liquid nitrogen to keep the temperature of the specimen below –160 °C for TEM imaging. After insertion of the specimen into the TEM, the specimen was allowed to stabilize for 10–20 minutes, typically to a temperature of –174 °C. During TEM imaging, the specimen temperature was monitored continuously by a cold stage controller (SmartSet 900, Gatan, Pleasanton, CA).

The images of the vitreous specimen were taken by an Eagle 2K CCD camera (FEI, Hillsboro, OR) mounted in the on-axis position of a Tecnai 12 TWIN transmission microscope (FEI, Hillsboro, OR) operated at 100 kV. Due to the high dynamic range and sensitivity of this camera, clear TEM micrographs were taken at extremely low electron-beam irradiation. This is critical in cryo-TEM imaging because high electron-beam radiation can cause the deformation and melting of the vitreous ice layer. The anti-contamination cryo-box of the TEM was charged with liquid nitrogen to minimize the contamination of specimen adjacent areas inside the TEM.

Table S1. Blotting and Plunging Parameters for Cryo-TEM

Parameter	Value
Blot time	1 s
Wait time [a]	0 s
Drain time [b]	0 s
Blot force [c]	2
Blot total [d]	1

[a] The time between blotting.

[b] Wait time between blotting and vitrification.

[c] Scale from 0 to 10 with the increment of 1.0.

[d] Number of blotting.

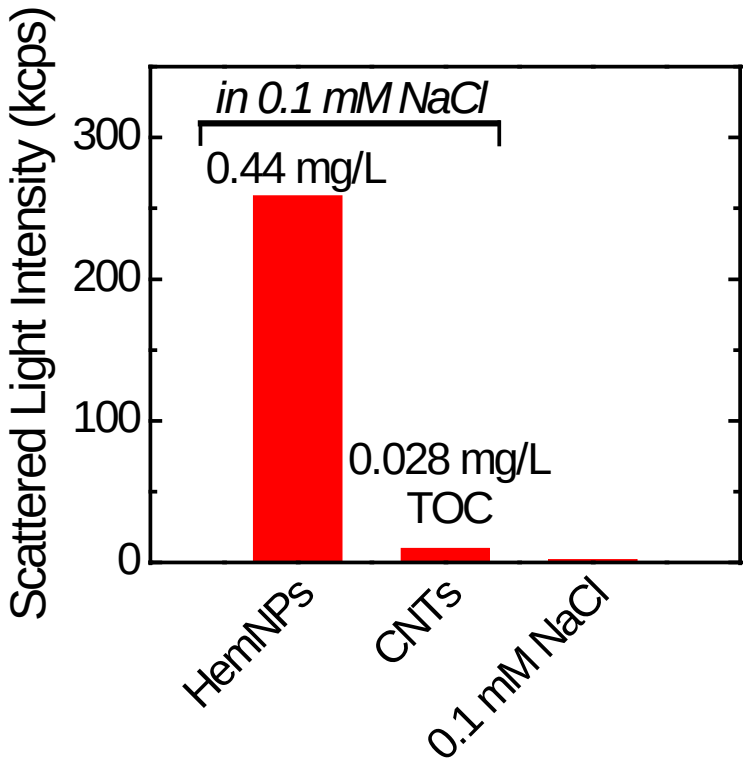

FIGURE S1. Scattered light intensities from HemNP suspension (0.44 mg/L), CNT suspension (27.82 µg/L TOC), and 0.1 mM NaCl solution at the same incident laser intensity (laser power of 2W). Intensities are presented in kilo counts per second (kcps).

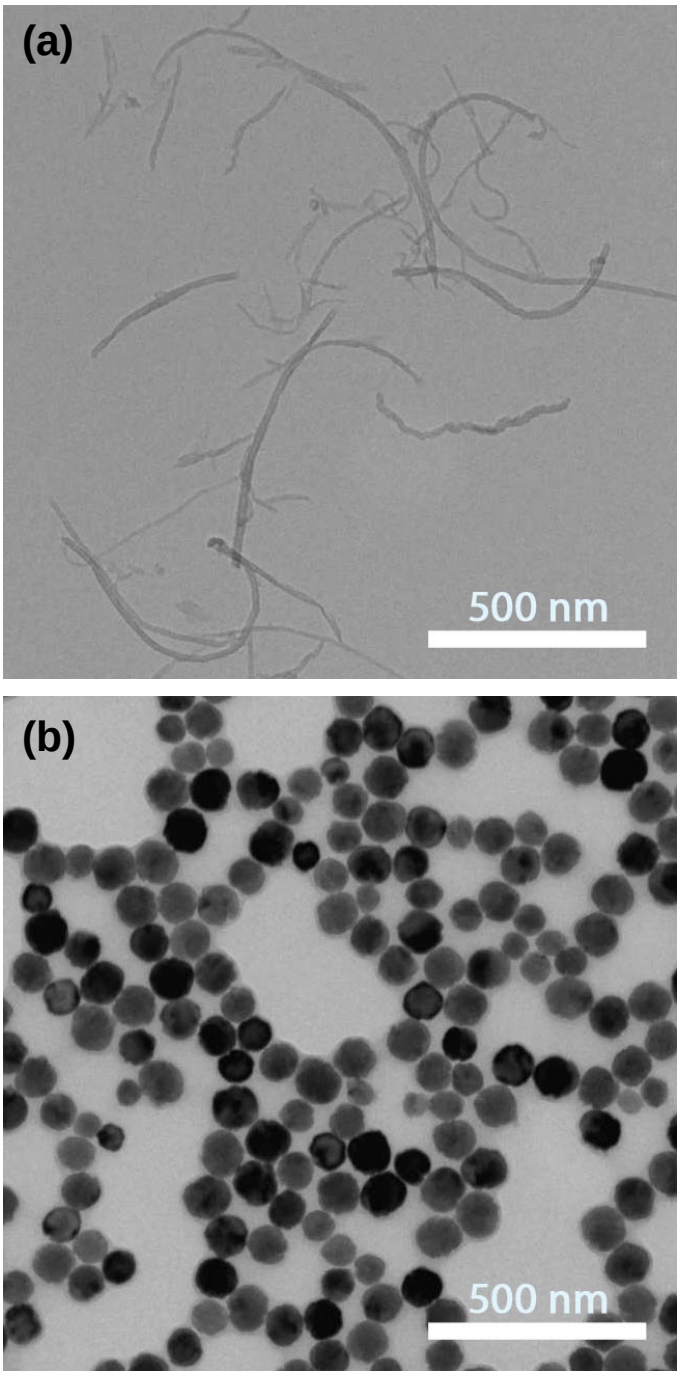

FIGURE S2. Representative TEM images of (a) CNTs and (b) HemNPs.

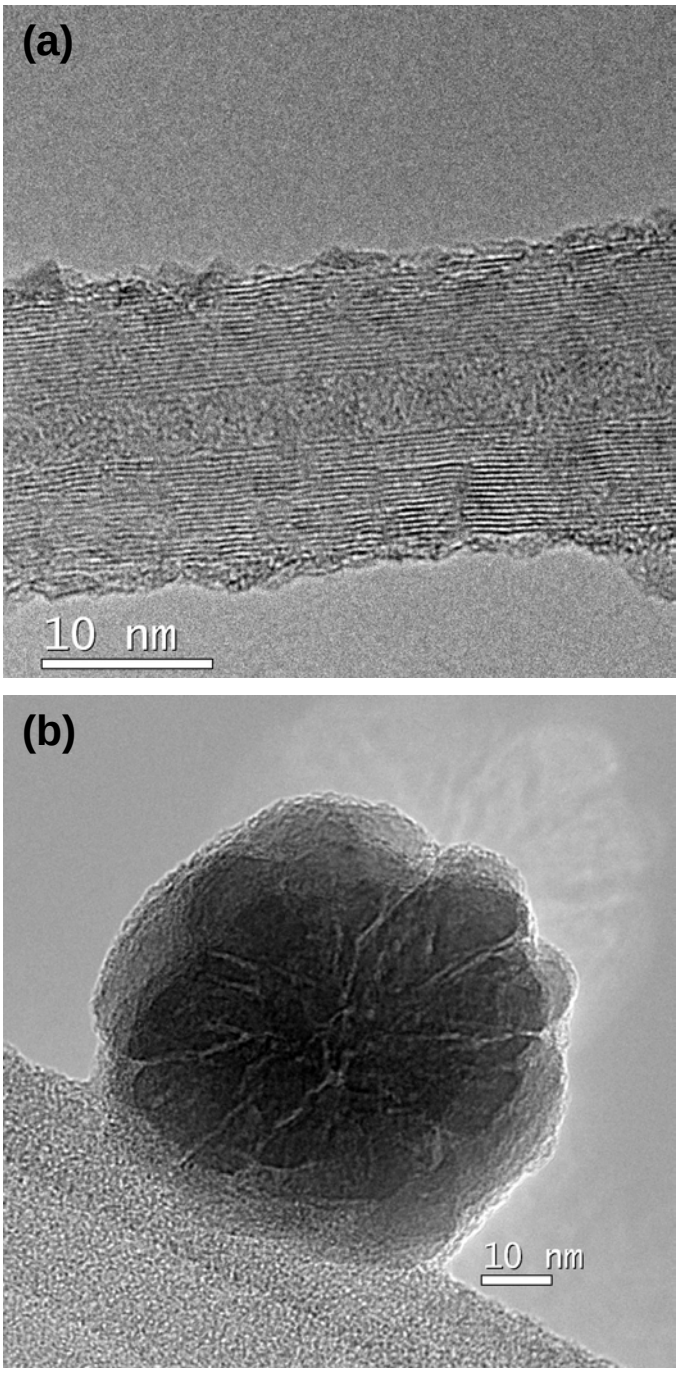

Figure S3. High-resolution TEM images of (a) a CNT and (b) a HemNP.

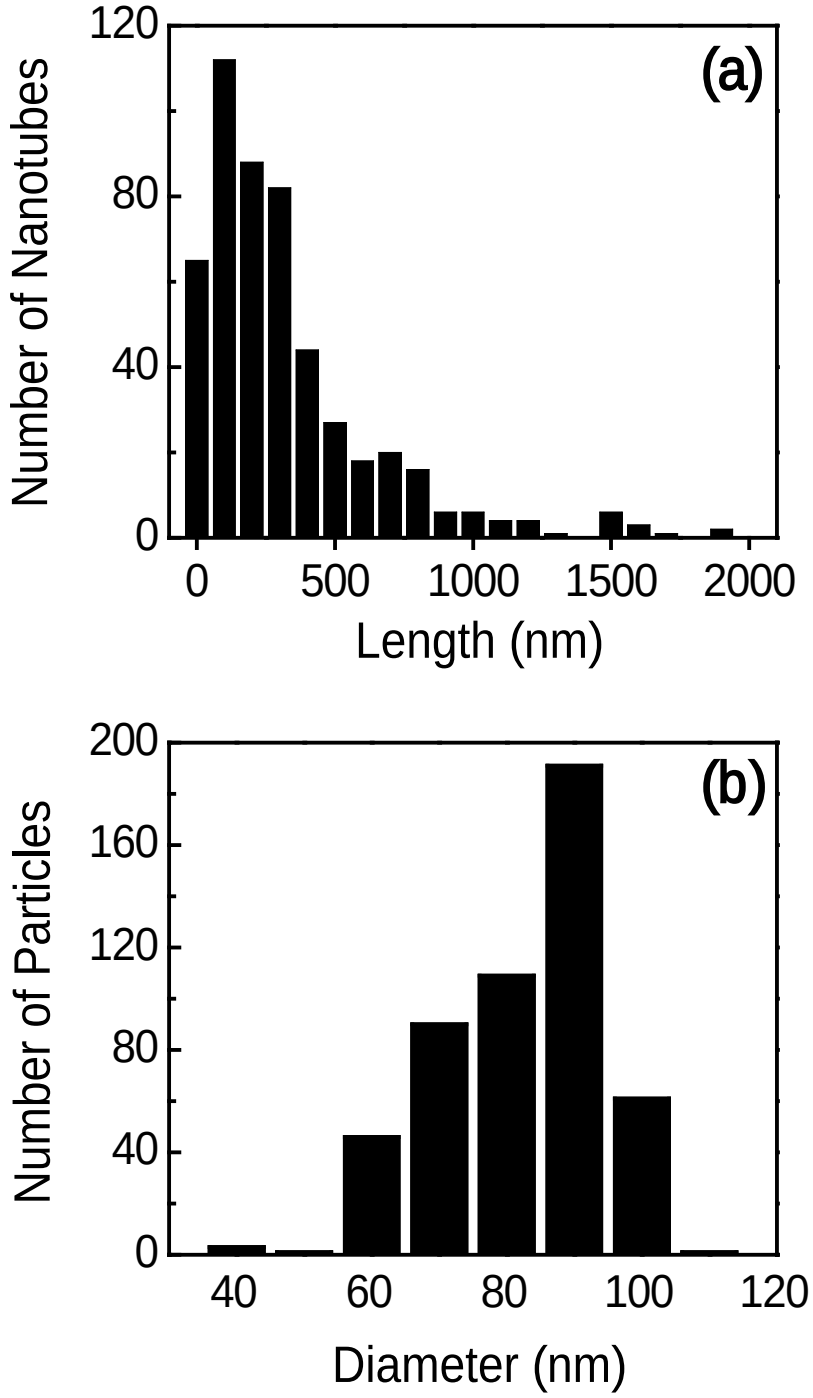

FIGURE S4. (a) Length distribution of CNTs with each bar representing a length range of 100 nm. (b) Size distribution of HemNPs with each bar representing a diameter range of 10 nm.

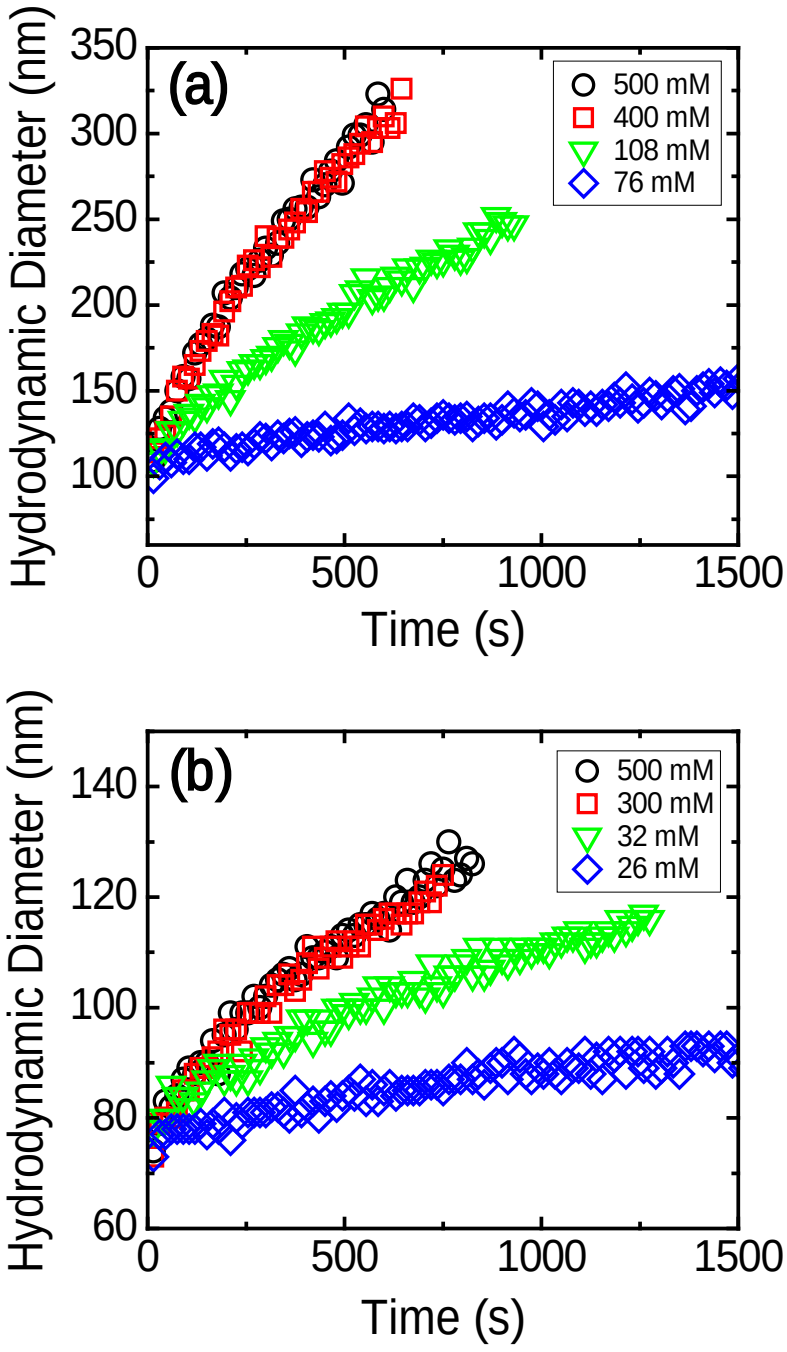

FIGURE S5. Representative homoaggregation profiles of (a) CNTs at a concentration of 83.46 µg/L TOC and (b) HemNPs at a concentration of 0.44 mg/L at different NaCl concentrations.

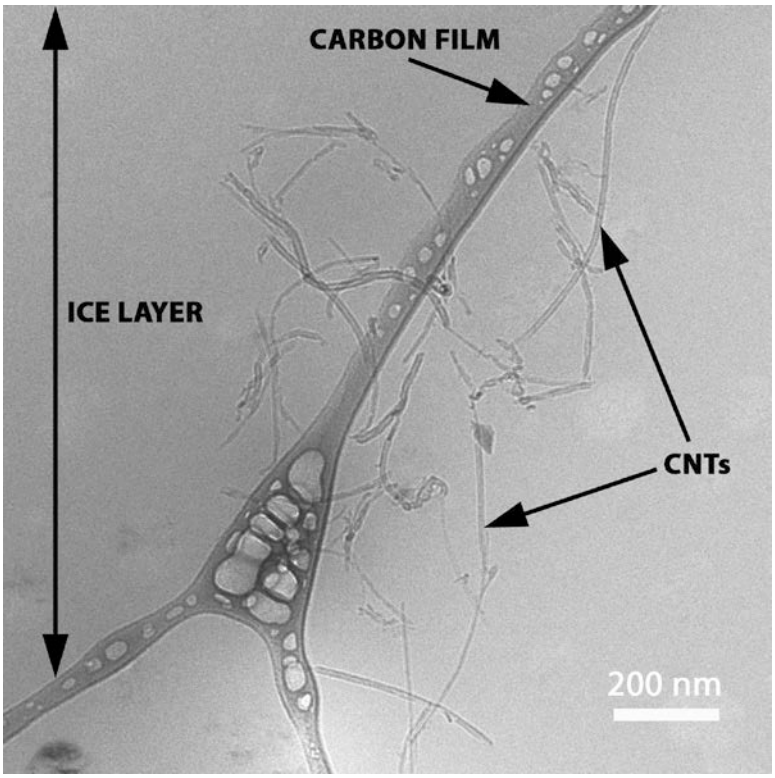

Figure S6. Cryo-TEM image of a CNT homoaggregate after 20 min of aggregation at 500 mM NaCl and pH 5.2. CNT concentration was 1.25 mg/L TOC.

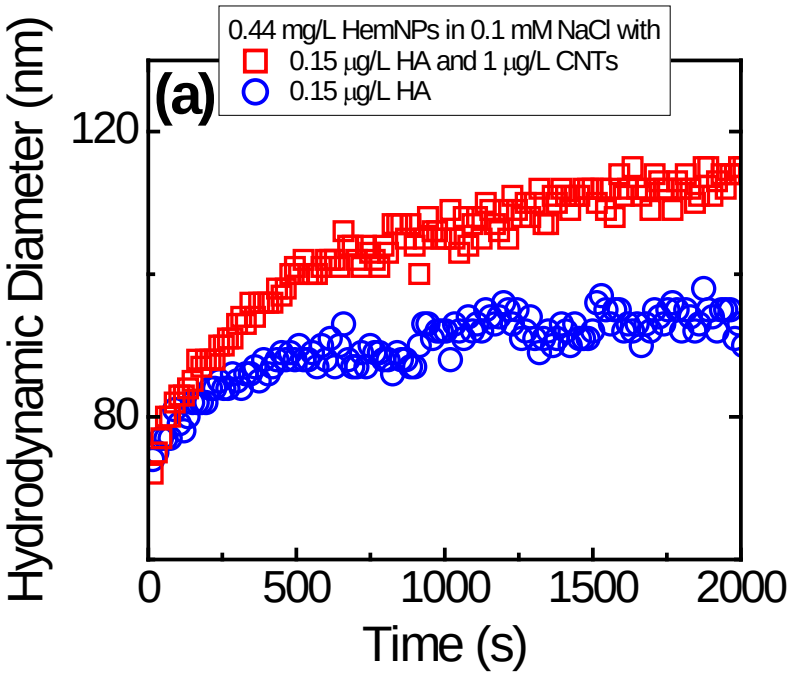
0.44 mg/L HemNPs in 0.1 mM NaCl with
0.15 μg/L HA and 1 μg/L CNTs
0.15 μg/L HA
(a)
Hydrodynamic Diameter (nm)
120
80
0
500
1000
1500
2000
Time (s)

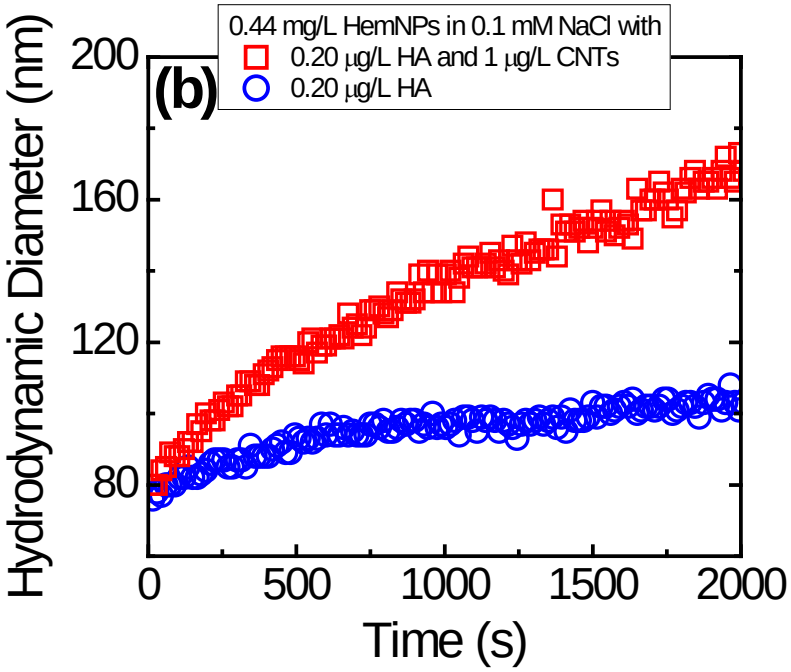
0.44 mg/L HemNPs in 0.1 mM NaCl with
0.20 μg/L HA and 1 μg/L CNTs
0.20 μg/L HA
(b)
Hydrodynamic Diameter (nm)
200
160
120
80
0
500
1000
1500
2000
Time (s)

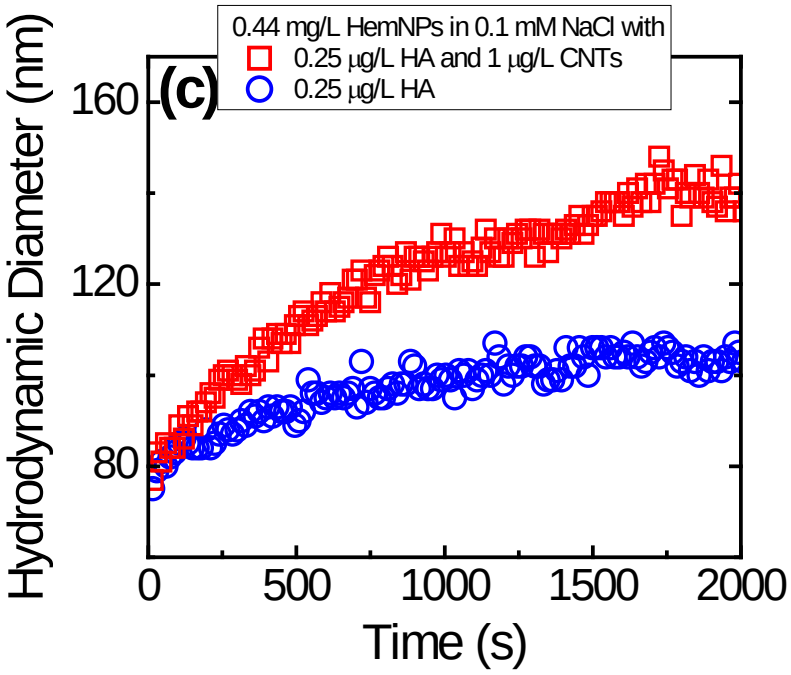

Figure S7. Influence of humic acid on the aggregation rates of HemNPs in the absence and presence of CNTs at 0.1 mM NaCl and pH 5.2. The humic acid concentrations are (a) 0.15 μg/L TOC, (b) 0.20 μg/L TOC, and (c) 0.25 μg/L TOC. For all experiments, the concentration of HemNPs is 0.44 mg/L. For experiments performed in the presence of CNTs, the CNT concentration is 1.11 μg/L TOC, resulting in a C/H ratio of 0.0025.

References

1. Yi, P.; Chen, K. L., Influence of Surface Oxidation on the Aggregation and Deposition Kinetics of Multiwalled Carbon Nanotubes in Monovalent and Divalent Electrolytes. *Langmuir* **2011,** 27, (7), 3588-3599.
2. Holthoff, H.; Egelhaaf, S.; Borkovec, M.; Schurtenberger, P.; Sticher, H., Coagulation rate measurements of colloidal particles by simultaneous static and dynamic light scattering. *Langmuir* **1996,** 12, (23), 5541-5549.
3. Chen, K. L.; Elimelech, M., Aggregation and Deposition Kinetics of Fullerene (C60) Nanoparticles. *Langmuir* **2006,** 22, (26), 10994-11001.
4. Chen, K. L.; Mylon, S. E.; Elimelech, M., Aggregation kinetics of alginate-coated hematite nanoparticles in monovalent and divalent electrolytes. *Environmental Science & Technology* **2006,** 40, (5), 1516-1523.
5. Huynh, K. A.; Chen, K. L., Aggregation Kinetics of Citrate and Polyvinylpyrrolidone Coated Silver Nanoparticles in Monovalent and Divalent Electrolyte Solutions. *Environmental Science & Technology* **2011**, (45), 5564-5571.